HAL
open science

Positron backscattering from solid targets: Modeling of scattering processes via various approaches

B. Kribaa, Z. Rouabah, C. Le Loirec, C. Champion, N. Bouarissa

To cite this version:

B. Kribaa, Z. Rouabah, C. Le Loirec, C. Champion, N. Bouarissa. Positron backscattering from solid targets: Modeling of scattering processes via various approaches. Micron, 2016, 87, pp.46-50. 10.1016/j.micron.2016.04.009 . cea-01845389

HAL Id: cea-01845389

https://cea.hal.science/cea-01845389

Submitted on 10 Jan 2019

HAL is a multi-disciplinary open access archive for the deposit and dissemination of scientific research documents, whether they are published or not. The documents may come from teaching and research institutions in France or abroad, or from public or private research centers.

L'archive ouverte pluridisciplinaire **HAL**, est destinée au dépôt et à la diffusion de documents scientifiques de niveau recherche, publiés ou non, émanant des établissements d'enseignement et de recherche français ou étrangers, des laboratoires publics ou privés.

Positron backscattering from solid targets: Modeling of scattering processes via various approaches

B. Kribaa [a], Z. Rouabah [a], C. Le Loirec [b], C. Champion [c], N. Bouarissa [d,*]

[a] Materials and Electronic Systems Laboratory (LMSE), University of Bordj Bou Arreridj, 34000 Bordj Bou Arreridj, Algeria
[b] CEA, LIST, F-91191 Gif-sur-Yvette, France
[c] Université de Bordeaux, CNRS/IN2P3, Centre d'Etudes Nucléaires de Bordeaux-Gradignan (CENBG), France
[d] Laboratory of Materials Physics and its Applications, University of M'sila, 28000 M'sila, Algeria

Monte Carlo simulation of 1–4 keV positron backscattering from semi-infinite solid targets ranging from Be (z = 4) to Au (z = 79) with normal angle of incidence is here reported. In our study, the elastic and inelastic scattering cross sections are modeled by using various approaches based on either a classical or a quantum mechanical treatment. Calculations of positron backscattering coefficient are then reported for the solid targets of interest. The results obtained show a fairly good agreement with the data available in the literature. The dependence of the positron backscattering coefficient versus the atomic number of the solid target of interest has been investigated. In this respect, polynomial functions are proposed which does not require any recourse to Monte Carlo calculations.

1. Introduction

Modeling the transport of low energy positrons in solid targets is of great importance for studying solid surfaces and defect profiles (Schultz and Lynn, 1988; Ishii, 1992; Puska and Nieminen, 1994; Dupasquier and Mills, 1995; Nieminen, 1995). Recent advances in this field have been directed towards understanding of the processes by which positrons slow down in solids. The ultimate fate of positrons in condensed matter is obviously annihilation in the nanosecond timescale. However, during that time a rich variety of physical phenomena occur whose knowledge is of prime importance for determining the particle ranges as well as the backscattering coefficients (Bouarissa et al., 1998; Bouarissa and Walker, 2000). With respect to the slow-positron-beam experiments, the essential point is that a large fraction of positrons can diffuse back to the surface and then be emitted into the vacuum either as free positron or as Positronium (Ps) (Boev et al., 1987). It is clear that the backscattering process must be sensitively determined by the details of the elastic and inelastic scattering interactions (Massoumi et al., 1992; Bouarissa and Al-Assiri, 2013). In this context, we refer the interested reader to the recent reviews and monographs dealing with positrons as condensed matter and near-surface probes (Schultz and Lynn, 1988; Ishii, 1992; Puska and Nieminen, 1994; Dupasquier and Mills, 1995; Nieminen, 1995). To study the penetration of charged particles in solids, the Monte-Carlo (MC) codes appears as the best-suited tools since able to model step by step, interaction after interaction the full history of the incident particle as well as that of all the secondary species created along the primary track in matter (Shimizu and Ze-Jun, 1992; Dapor, 1991, 1992, 2003; Sobol, 1975; Jensen et al., 1990; Rouabah et al., 2015). Thus, by comparing the parameters obtained from the Monte Carlo simulation with experiments, one can get information about the accuracy of the modeling of the scattering processes used in the simulation.

The current work aims at studying backscattering of 1–4 keV positrons from solid targets ranging from Be to Au. To do that, the modeling of elastic and inelastic scattering cross sections was provided by using a variety of classical and quantum approaches. As an application, positron backscattering coefficients have been determined for a large set of solid targets including materials such as Ti, Fe, and Sn, which have never been investigated, to the best of or knowledge. Comparisons with experiment show a fairly good

* Corresponding author.
E-mail address: n_bouarissa@yahoo.fr (N. Bouarissa).

agreement and point out the accuracy of both the classical and the quantum mechanical approaches.

2. Theoretical details

In the first approach used in the present work and referred to as PW1, the elastic scattering is modeled by using the Rutherford differential cross section, modified to account the electronic screening (Valkealahti and Nieminen, 1983), where the numerical coefficient in the Nigam atomic screening factor is taken to be a variable that depends on the positron energy before each collision, as suggested by Bouarissa et al. (1998). In this respect, the numerical coefficient in the Nigam atomic screening factor referred to as μ (Bouarissa et al., 1998) has been determined for several selected solid targets ranging from Be to Au in the positron primary energy range of 1–4 keV. Our results give the following expressions:

$$\mu(E) = -0.305 \times 10^{-10} E^3 + 0.2517 \times 10^{-6} \mathrm{E}^2 - 0.0007\mathrm{E} + 3.258 \quad (for\ Be) \tag{1}$$

$$\mu(E) = -1.44 \times 10^{-10} E^3 + 1.32 \times 10^{-6} \mathrm{E}^2 - 0.0042\mathrm{E} + 9.23 \quad (for\ Al + Si) \tag{2}$$

$$\mu(E) = -1.82 \times 10^{-10} E^3 + 1.586 \times 10^{-6} \mathrm{E}^2 - 0.00488\mathrm{E} + 9.455 \quad (for\ Ti) \tag{3}$$

$$\mu(E) = -2.49 \times 10^{-10} E^3 + 2.285 \times 10^{-6} \mathrm{E}^2 - 0.00745\mathrm{E} + 14.27 \quad (for\ Fe) \tag{4}$$

$$\mu(E) = -3.35 \times 10^{-10} E^3 + 3.20 \times 10^{-6} \mathrm{E}^2 - 0.011\mathrm{E} + 22.26 \quad (for\ Cu) \tag{5}$$

$$\mu(E) = -1.9 \times 10^{-10} E^3 + 1.94 \times 10^{-6} \mathrm{E}^2 - 0.00754\mathrm{E} + 17.83 \quad (for\ Zn) \tag{6}$$

$$\mu(E) = -1.69 \times 10^{-10} E^3 + 0.4059 \times 10^{-6} \mathrm{E}^2 - 0.00336\mathrm{E} + 14.97 \quad (for\ Sn) \tag{7}$$

$$\mu(E) = -1.46 \times 10^{-10} E^3 + 1.82 \times 10^{-6} \mathrm{E}^2 - 0.009\mathrm{E} + 23.18 \quad (for\ Au) \tag{8}$$

For inelastic processes, both core and valence electron excitations are treated by using Gryzinski excitation function expressions (Gryzinski, 1965a,b,c). To calculate the total inelastic scattering cross section, we have followed the procedure of Bouarissa described in details in Bouarissa (1987).

In the second approach used in the present work (referred to as PW2), the elastic scattering is treated by using the analytical approximation as independently developed by Baro et al. (1994, 1995) and by Miotello and Dapor (1997). In this approximation, the transport cross-section has been calculated for each target element of interest using the approximation of Rouabah et al. (2009). Similarly to the first approach of the present contribution, the inelastic scattering has been treated using Gryzinski excitation function expressions as described by Bouarissa (1987).

The third approach used in the present work (referred to as PW3) consists in treating the elastic scattering by using the same method as that described in the second approach of this contribution, whereas the inelastic scattering has been handled by substituting the Gryzinski's formula, in our Monte Carlo code with the Ashley's differential inverse inelastic mean free path as described in Ashley's optical-model (Ashley, 1988, 1990). Finally, the fourth approach used in the present work (referred to as PW4) is based on the PENELOPE code. The latter is a Monte Carlo code of general purpose that permits us to simulate the coupled transport of photons, electrons and positrons in matter with a very good accuracy at low energies (Salvat et al., 2006; Sempau et al., 2003). The electrons and positrons are simulated using a mixed scheme where interactions are classified into hard and soft. Hard events are simulated step by step and involve angular deflection or energy losses above user-defined cutoffs whereas soft events occurring between two hard collisions are simulated by means of an artificial single event. We used the 2006 release of the code (Salvat et al., 2006).

3. Simulation procedure

The Monte Carlo simulation is probably the most powerful theoretical method for investigating the charged-particle-solid interaction problem. Besides, it also provides a physical insight of the details of the investigation process in addition to their results. Initially positrons lose rapidly their energy in a solid target. Energy is lost to electron excitations, including target atom ionizations and collective plasmon-like processes. Phonon excitations take over at lower energies, which eventually lead to positron thermalization (Puska and Nieminen, 1994). The thermal stage ends when the positron annihilates with an electron. The basic idea of the Monte Carlo simulation is to simulate trajectories of the positron penetrating into solid targets. The positron-host atom interaction is incorporated into the Monte Carlo framework via the cross sections for the different scattering processes. The simulation uses uniform random numbers belonging to the range [0–1].

In the present paper, a Monte Carlo simulation program that has essentially the same general structure as that of Bouarissa (1987) has been used for the PW1, PW2 and PW3 approaches. In all cases, we follow the positron until its energy becomes smaller than an energy cut-off here taken to be 20 eV. As a matter of fact, the choice of this energy does not have much effect, since the path length travelled by the positron between 20 eV and near thermal energy is insignificant compared to the implantation depth (Baker et al., 1991). All results obtained from these approaches are for semi-infinite medium with a planar surface with normal incidence of the positrons. 10^4 particle histories are used in each simulation run for each system.

As regards the PW4 approach, the simulation is controlled by parameters fixed for the various materials used in the geometry:

(i) E_{abs} is the absorption energy, namely, the energy at which the track evolution is stopped. The kinetic energy of the particle is then locally deposited.
(ii) C_1 is the average angular deflection between two hard elastic collisions.
(iii) C_2 is the maximal fractional energy loss between two hard elastic collisions.
(iv) W_{CC} is the energy cut-off for hard inelastic interactions.
(v) W_{CR} is the energy cut-off for hard bremsstrahlung emission. We used the 2006 release of the code (Salvat et al., 2006).

The TABLES.F program, which produces tables of interaction properties for arbitrary materials is used to determine the positron range and stopping powers in the different investigated materials. A complete simulation is performed to get the backscattering

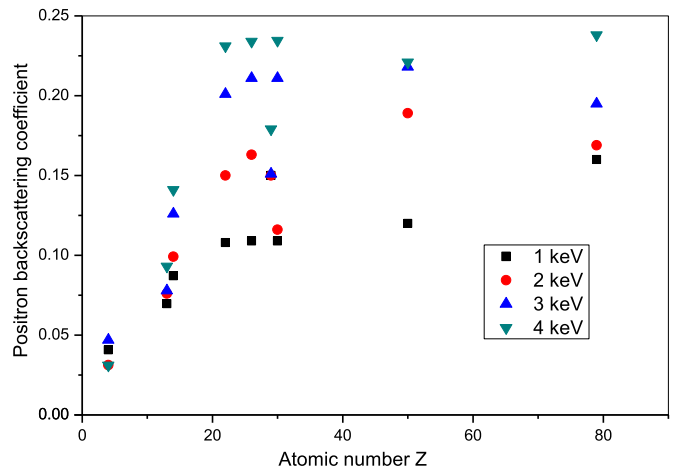

Fig. 1. Positron backscattering coefficient as a function of the atomic number of solid targets.

Table 1
Backscattering coefficients of 1–4 keV positrons impinging in semi-infinite Al target.

Energy (keV)	Al				Exp[a]	Theo[b]	Theo[c]
	PW1	PW2	PW3	PW4			
1	0.0697	0.076	0.078	0.0814	0.069	0.086	0.109
2	0.076	0.081	0.076	0.0965		0.099	
3	0.0779	0.085	0.088	0.108	0.086	0.107	0.115
4	0.093	0.0852	0.113	0.111		0.112	

[a] Coleman et al. (1992).
[b] Jensen and Walker (1993).
[c] Dapor (1996).

Table 2
Backscattering coefficients of 1–4 keV positrons impinging in semi-infinite Cu target.

Energy (keV)	Cu				Exp[a]	Theo[c]
	PW1	PW2	PW3	PW4		
1	0.150	0.172	0.184	0.0895	0.135	0.156
2	0.150	0.162	0.173	0.138		
3	0.151	0.161	0.168	0.160	0.194	0.1194
4	0.179	0.170	0.172	0.179		

[a] Coleman et al. (1992).
[c] Dapor (1996).

Table 3
Backscattering coefficients of 1–4 keV positrons impinging in semi-infinite Be and Si targets.

Energy (keV)	Be		Theo[c]	Si	
	PW1	PW4		PW1	PW4
1	0.0408	0.0346	0.042	0.0871	0.0881
2	0.0312	0.0326		0.0992	0.107
3	0.0470	0.0351	0.038	0.126	0.116
4	0.0310	0.0301		0.141	0.125

[c] Dapor (1996).

Table 4
Backscattering coefficients of 1–4 keV positrons impinging in semi-infinite Ti and Fe targets.

Energy (keV)	Ti		Fe	
	PW1	PW4	PW1	PW4
1	0.108	0.104	0.109	0.0964
2	0.150	0.160	0.163	0.141
3	0.201	0.191	0.211	0.155
4	0.231	0.223	0.234	0.170

coefficient of each material. Primary positrons impinge normally on semi-infinite material slabs with a given energy (from 1 to 4 keV). We used the same parameters as those reported by Sempau et al. (2003) in their benchmark of PENELOPE. E_{abs} for positrons is set equal to 0.05% of the beam energy. In all cases, W_{CC} and W_{CR} are equal to E_{abs} (positron) and E_{abs} (photon), respectively. For photons, we set E_{abs} equal to one tenth of the incident beam energy. The parameters C_1 and C_2 are set equal to 0.05. The backscattering coefficients are calculated by the code.

4. Results

Many of the positrons implanted in the primary beam may reach the entrance surface prior to their annihilation, either before or after thermalization. Several scenarios are then possible (Puska and Nieminen, 1994, 1995). The versatility of scenarios implies that positrons can be used to extract useful information of material properties near surfaces and interfaces. Besides, backscattering coefficients of positrons impinging on solid targets may provide stringent tests on the accuracy of the description of the scattering processes.

In the present work, the backscattering coefficients for 1–4 keV positron backscattered from semi-infinite selected target materials ranging from Be (z = 4) to Au (z = 79) have been calculated at normal incidence using the Monte Carlo simulation technique. Our results obtained using the different mentioned approaches, namely, PW1, PW2, PW3 and PW4 are given in Tables 1–6. Also shown for comparison are the experimental and previous theoretical data available in the literature. Note that the present calculated positron backscattering coefficients regarding the various materials of interest obtained using the different approaches are generally in reasonably good agreement with the experimental data reported in Coleman et al. (1992). In terms of theoretical calculations, our results agree generally well with those reported in Dapor (1996) and Jensen and Walker (1993). When comparing between the different approaches used in the present contribution, one can note that the values of the positron backscattering coefficients obtained from the PW1, PW2 and PW3 approaches based on the classical treatment are generally close to those calculated from the PW4 approach based on the quantum treatment. Furthermore, the PW1, PW2 and PW3 values are in some cases better than those of PW4 as compared to experiment. This suggests that the approaches used in the calculation of the elastic and inelastic scattering cross sections and the stochastically description of positron transport implied by the Monte Carlo method are compatible with the experiments. It should be noted that for some solid targets of interest, no comparison has been made with the experimental or previous theoretical

Table 5
Backscattering coefficients of 1–4 keV positrons impinging in semi-infinite Zn and Sn targets.

Energy (keV)	Zn		Exp[a]	Sn	
	PW1	PW4		PW1	PW4
1	0.090	0.0925	0.089	0.120	0.108
2	0.116	0.131		0.189	0.151
3	0.132	0.156	0.125	0.218	0.187
4	0.155	0.174		0.221	0.241

[a] Coleman et al. (1992).

Table 6
Backscattering coefficients of 1–4 keV positrons impinging in semi-infinite Au target.

Energy (keV)	Au				Exp[a]	Theo[b]	Theo[c]
	PW1	PW2	PW3	PW4			
1	0.160	0.090	0.154	0.105	0.123	0.111	0.168
2	0.159	0.142	0.174	0.152		0.156	
3	0.195	0.167	0.195	0.196	0.186	0.186	0.240
4	0.238	0.190	0.208	0.221		0.208	

[a] Coleman et al. (1992).
[b] Jensen and Walker (1993).
[c] Dapor (1996).

data in the literature. In these cases, our results are predictions and may serve for reference for future works. Interestingly as well, one notes that the positron backscattering coefficient depends on both the solid target and the positron primary energy. Generally, the positron backscattering coefficient increases with increasing its primary energy for all elements of interest. The behavior is almost most common for all used approaches (classical and quantum ones) in the current work. Furthermore, it is consistent with the results of the previous theoretical models of positron implantation in solid targets (Dapor, 1996; Jensen and Walker, 1993) as well as with the available experimental data reported in the literature (Coleman et al., 1992) within the experimental uncertainty. It is to be noted that the positron backscattering coefficient is much smaller than the electrons backscattering coefficient (Hannachi et al., 2014). This can be traced back to the difference of the elastic scattering cross section of crystal atoms for positrons and electrons.

In Fig. 1 we show the variation of the positron backscattering coefficient denoted by η versus the atomic number z of the solid targets of interest for various positron primary energies in the range 1–4 keV obtained from the PW4 approach. In this respect, we have tentatively suggested expressions that give the dependence of the positron backscattering coefficient on z for all solid targets under investigation in the following form:

$$E = 1\,\text{keV}$$

$$\eta(z) = 7.79 \times 10^{-7} z^3 - 1.17 \times 10^{-4} z^2 + 0.55 \times 10^{-2} z + 0.022 \quad (9)$$

$$E = 2\,\text{keV}$$

$$\eta(z) = 1.48 \times 10^{-6} z^3 - 2.24 \times 10^{-4} z^2 + 1.04 \times 10^{-2} z + 0.002 \quad (10)$$

$$E = 3\,\text{keV}$$

$$\eta(z) = 1.51 \times 10^{-6} z^3 - 2.33 \times 10^{-4} z^2 + 1.15 \times 10^{-2} z - 0.004 \quad (11)$$

$$E = 4\,\text{keV}$$

$$\eta(z) = 1.73 \times 10^{-6} z^3 - 2.72 \times 10^{-4} z^2 + 1.37 \times 10^{-2} z - 0.017 \quad (12)$$

Table 7
Coefficients a(E), b(E), c(E) and d(E) for each positron incident energy in the range 1–4 keV.

Positron incident energy (keV)	a(E)	b(E)	c(E)	d(E)
1	7.79×10^{-7}	-1.17×10^{-4}	0.55×10^{-2}	0.022
2	1.48×10^{-6}	-2.24×10^{-4}	1.04×10^{-2}	0.002
3	1.51×10^{-6}	-2.33×10^{-4}	1.15×10^{-2}	−0.004
4	1.73×10^{-6}	-2.72×10^{-4}	1.37×10^{-2}	−0.017

Equations (9)–(12) are generalized and expressed as,

$$\eta(z, E) = a(E) \times z^3 + b(E) \times z^2 + c(E) \times z + d(E) \quad (13)$$

The determined coefficients a(E), b(E), c(E) and d(E) are summarized in Table 7. In view of this table, it seems that the coefficients a(E) and c(E) increase with increasing the positron primary energy from 1 up to 4 keV which is not the case for b(E) and d(E) that decrease when increasing the positron primary energy.

Equations (9)–(13) provide the prediction of low-energy positron backscattering coefficients for a large set of solid targets ranging from Be (z = 4) to Au (z = 79) without requiring any recourse to the Monte Carlo calculations.

5. Conclusion

A Monte Carlo simulation of positron slowing down in selected solid targets ranging from Be to Au in the primary energy range 1–4 keV has been performed. Various approaches based on both classical and quantum treatments have been used for describing the elastic and inelastic scattering cross sections. Our results in terms of positron backscattering coefficient show that all used approaches give results that are in reasonably good agreement with the available experimental and previous theoretical data reported in the literature. It is found that the positron backscattering coefficient versus the atomic number z of the materials of interest can be fitted with polynomial functions for given positron primary energies within the range 1–4 keV.

References

Ashley, J.C., 1988. Interaction of low-energy electrons with condensed matter: stopping powers and inelastic mean free paths from optical data. Electron Spectros. Relat. Phenom. 46, 199–214.
Ashley, J.C., 1990. Energy loss rate and inelastic mean free path of low-energy electrons and positrons in condensed matter. J. Electron Spectros. Relat. Phenom. 50, 323–334.
Baker, J.A., Chilton, N.B., Jensen, K.O., Walker, A.B., Coleman, P.G., 1991. Median penetration depths and implantation profiles for low energy positrons in Al. J. Phys. Condens. Matter 3, 4109–4114.
Baro, J., Sempau, J., Fernández-Varea, J.M., Salvat, F., 1994. Simplified Monte Carlo simulation of elastic electron scattering in limited media. Nucl. Instrum. Methods Phys. Res. B 84, 465–483.
Baro, J., Sempau, J., Fernández-Varea, J.M., Salvat, F., 1995. An algorithm for Monte Carlo simulation of the penetration and energy loss of electrons and positrons in matter. Nucl. Instrum. Methods Phys. Res. B 100, 31–46.
Boev, O.V., Puska, M.J., Nieminen, R.M., 1987. Electron and positron energy levels in solids. Phys. Rev. B 36, 7786–7794.
Bouarissa, N., 1987. Monte Carlo Simulation of Positron Penetration in Metals. University of East Anglia, Norwich, UK (Thesis).
Bouarissa, N., Al-Assiri, M.S., 2013. Transport of electrons and positrons impinging on solid targets: a comparative study performed by using a Monte Carlo simulation. J. Electron Spectrosc. Relat. Phenom. 191, 11–15.
Bouarissa, N., Walker, A.B., 2000. A computer simulation of slow positron implantation depths in aluminium. Intern. J. Mod. Phys. B 14, 1603–1612.
Bouarissa, N., Walker, A.B., Aourag, H., 1998. Backscattering of slow positron from semi-infinite aluminium. J. Appl. Phys. 83, 3643–3648.
Coleman, P.G., Albrecht, L., Jensen, K.O., Walker, A.B., 1992. Positron backscattering from elemental solids. J. Phys.: Condens. Matter 4, 10311–10322.
Dapor, M., 1991. Monte Carlo simulation of the energy deposited by few keV electrons penetrating in thick targets. Phys. Lett. A 158, 425–430.
Dapor, M., 1992. Monte Carlo simulation of backscattered electrons and energy from thick targets and surface films. Phys. Rev. B: Condens. Matter 46, 618–625.
Dapor, M., 1996. Elastic scattering calculations for electrons and positrons in solid targets. J. Appl. Phys. 79, 8406–8411.

Dapor, M., 2003. Electron-Beam Interactions With Solids: Application of the Monte Carlo Method to Electron Scattering Problems. Springer, Berlin.
Dupasquier, A., Mills, A.P. (Eds.), 1995. Positron Spectroscopy of Solids. IOS Press, Amsterdam.
Gryzinski, M., 1965a. Two-particle collisions I. General relations for collisions in the laboratory system. Phys. Rev. 138, A305–A321.
Gryzinski, M., 1965b. Two particle collisions II. Coulomb collision in the laboratory system coordinates. Phys. Rev. 138, A322–A336.
Gryzinski, M., 1965c. Classical theory of atomic collision I. Theory of inelastic collisions. Phys. Rev. 138, A336–A358.
Hannachi, M., Rouabah, Z., Champion, C., Bouarissa, N., 2014. Electron backscattering from solid targets: elastic scattering calculations. J. Electron Spectrosc. Relat. Phenom. 195, 155–159.
Ishii, A., 1992. Positrons at Metallic Surfaces. Trans Tech. Publications, Switzerland.
Jensen, K.O., Walker, A.B., Bouarissa, N., 1990. Positron beams for solids and surfaces. In: Schultz, P.J., Massoumi, G.R., Simpson, P.J. (Eds.), AIP Conf. Proc., 218. American Institute of Physics, New York, pp. 19–28.
Jensen, K.O., Walker, A.B., 1993. Monte Carlo simulation of the transport of fast electrons and positrons in solids. Surf. Sci. 292, 83–97.
Massoumi, G.R., Hozhabri, N., Jensen, K.O., Lennard, W.N., Lorenzo, M.S., Schultz, P.J., Walker, A.B., 1992. Positron and electron backscattering from solids. Phys. Rev. Lett. 68, 3873–3876.
Miotello, A., Dapor, M., 1997. Slow electrons impinging on dielectric solids. II. Implantation profiles electron mobility, and recombination processes. Phys. Rev. B: Condens. Matter 56, 2241–2247.
Nieminen, R.M., 1995. Mat. Sci. Forum 175–178, 279–286.
Puska, M.J., Nieminen, R.M., 1994. Theory of positrons in solids and on solid surfaces. Rev. Mod. Phys. 66, 841–893.
Rouabah, Z., Bouarissa, N., Champion, C., Bouaouadja, N., 2009. Study on electron scattering in solid targets using accurate transport cross-sections. Appl. Surf. Sci. 255, 6217–6220.
Rouabah, Z., Hannachi, M., Champion, C., Bouarissa, N., 2015. Monte Carlo simulation of electron slowing down in indium. J. Electron Spectrosc. Relat. Phenomena 202, 7–15.
Salvat, F., Fernández-Varea, J.M., Sempau, J., 2006. PENELOPE-A Code System for Monte Carlo Simulation of Electron and Photon Transport. OECD Nuclear Energy Agency, Issy-Les-Moulineaux, France.
Schultz, P.J., Lynn, K.G., 1988. Interaction of positron beams with surfaces thin films, and interfaces. Rev. Mod. Phys. 60, 701–773.
Sempau, J., Fernández-Varea, J.M., Acosta, E., Salvat, F., 2003. Experimental benchmarks of the Monte Carlo code PENELOPE. Nucl. Instrum. Meth. Res. B 207, 107–123.
Shimizu, R., Ze-Jun, D., 1992. Monte Carlo modelling of electron-solid interactions. Rep. Prog. Phys. 55, 487–531.
Sobol, I.M., 1975. The Monte Carlo Method. MIR, Moscou, pp. 38–62.
Valkealahti, S., Nieminen, R.M., 1983. Monte Carlo calculations of keV electron and positron slowing down in solids. Appl. Phys. A 32, 95–106.